Mine Water and the Environment (2019) 38:294–309
https://doi.org/10.1007/s10230-019-00591-8

TECHNICAL ARTICLE

Sensitivity of Percolation Estimates to Modeling Methodology: A Case Study at an Unlined Tailings Facility with Limited Monitoring Data

Spencer K. Whitman[1] · **Ronald J. Breitmeyer**[1]

Received: 22 January 2018 / Accepted: 11 January 2019 / Published online: 18 January 2019

Abstract

Calculation of water budgets is critical to developing long-term management and remediation plans for legacy mine waste facilities. The effects of several modeling decisions commonly made by practitioners constructing numerical hydrologic models can significantly alter estimates of percolation and resultant management strategies. We investigated the effects of variations in several common modeling decisions for an unlined legacy tailings emplacement in Lincoln County, Nevada using predictions from HYDRUS 1D and 2D simulations. Modeling decisions investigated include choice of hydraulic property model, hydraulic properties, numerical mesh discretization, boundary condition representation, dimensionality, and geometry. Hydrologic parameterization was informed by measurement of field-saturated hydraulic conductivity, in-situ density, field moisture content, bulk (dry) density, and water retention curve by hanging column, pressure plate, and chilled mirror hygrometer. Numerical hydrologic models resulted in percolation estimates from 0 to 24 mm/year through the tailings. Choice of hydraulic properties and temporal resolution of boundary condition data contributed the most to variations in percolation estimates. For comparison, percolation was predicted with a simple water balance model (HELP), resulting in a percolation rate of 51 mm/year. Such a wide range of percolation rate predictions demonstrates the potential for significant variability in model output within a range of defensible modeling decisions, assumptions, and parameterization methods. To appropriately bound this uncertainty, several model assumptions and iterations should be considered.

Keywords Vadose · Unsaturated · Water balance · Drainage · Closure · Reclamation · Hydrus · Modeling · Simulation · Mine waste

Introduction

Management of leachate solutions from mine waste materials such as tailings or waste rock is a long-term environmental concern as these leachates often contain concentrations of solutes that exceed statutory limits (Jung 2001; Moore and Luoma 1990; Salomons 1995). The problem of leachate or solution management is compounded on legacy sites where containment, treatment, and/or monitoring infrastructure is absent or inadequately engineered (Navarro et al. 2008; Younger et al. 2002).

Leachate solutions are typically composed of residual moisture and meteoric water that percolates through mine waste materials, potentially leaching parameters of concern (PoCs) into the environment. Movement of PoCs through the vadose zone to groundwater and subsequent degradation of groundwater resources is a primary long-term concern. Models provide a means of assessing the potential production and subsequent migration of PoCs through the vadose zone to groundwater.

In this study, models for predicting percolation are split into two categories. Numerical hydrologic models such as HYDRUS 1D and 2D (Šimůnek et al. 2012, 2013) are those that solve the Richards equation (Richards 1931) using numerical methods, while simplified models use a combination of empirical relationships, defining equations, and mass balance approaches to estimate percolation. Simplified models such as the Hydrologic Evaluation of Landfill Performance (HELP) model (Schroeder et al. 1994) are typically conservative (i.e. they over-predict percolation), and provide a semi-quantitative assessment of water budgets, but do not consider the full range of processes governing the fate and transport of PoCs (Berger 2000). Full consideration

✉ Spencer K. Whitman
swhitman@nevada.unr.edu

[1] Department of Geological Sciences and Engineering, University of Nevada Reno, Reno, NV 89557, USA

of the governing processes is critical to understanding risks to natural resources. Increased physical representativeness typically requires additional model parameterization, modeling decisions, assumptions, and knowledge of numerical methods (Anderson and Woessner 1992). The increased parameterization requirements of complicated models are particularly problematic on sites with limited data.

The objective of this study was to investigate the effects that common variations in modeling methodology have on developing bounding estimates of percolation for data-limited sites. Variation in predictions from numerical hydrologic models was assessed by varying choice of unsaturated hydraulic property model, hydraulic properties, finite element mesh discretization, upper and lower boundary conditions, and model dimensionality and geometry in a series of HYDRUS 1D and 2D simulations. Variations due to process simulation are represented by comparison of percolation predictions from HELP and HYDRUS simulations that were constructed in an identical manner. While textbooks are available for guidance on numerical modeling of unsaturated flow (Morel-Seytoux 1989; Radcliffe and Šimůnek 2010; Rassam et al. 2003; Szymkiewicz 2013), no case studies documenting the effects of common modeling decisions for numerical model of unsaturated flow are currently available. This study is intended to be a resource for practitioners and regulators by illuminating the modeling decisions that will most affect percolation estimates.

Site Background

Location, Geography, and Climate

The site considered in this study is the Caselton Wash Tailings, located in Lincoln County, NV, approximately 275 km north of Las Vegas (Fig. 1). Geography at the site consists of north to northwest trending mountain ranges separated by arid sedimentary basins. Elevation on the tailings surface ranges from 1720–1795 masl.

Climate data for Pioche, NV were gathered from the Western Regional Climate Center (2016) for the period 1945 to 2005. Temperatures ranged from − 23 to 38 °C, while

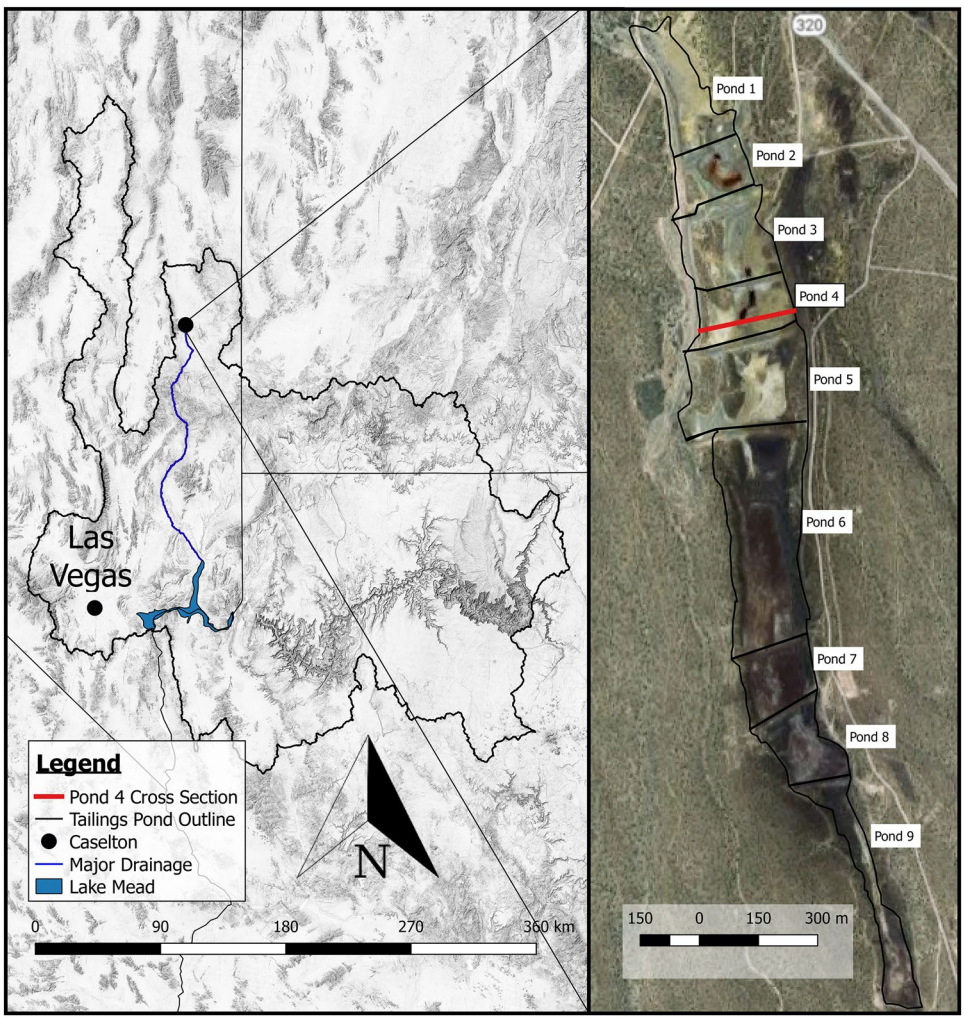

Fig. 1 Location map for the Caselton Wash tailings

monthly averaged daily minimum temperatures ranged from − 6 °C in January to 15 °C in July, and monthly averaged daily maximum temperatures ranged from 6 °C in January to 31 °C in July. Annual precipitation totals were approximately 35 cm, consisting of mixed snow and rain from December to March and episodic convective storms from April through November (Fig. 2).

Caselton Wash Tailings

Tailings from the Caselton Mill were deposited ~ 1.3 km to the southwest in an unlined alluvial channel (Caselton Wash) from the early 1900s through the 1960s. The disposal of tailings in Caselton Wash has created a potential source for soil and groundwater contamination beneath the tailings. Caselton Wash is a major drainage feature, incised about 21 m into a pediment of Quaternary alluvium. Caselton Wash tailings consists of 10 earthen dams that contain nine separate tailings ponds. Ponds are numbered 1–9 from the topographically highest to lowest (Fig. 1). Ponds 1–4 are composed of acid generating tailings derived from sulfide ore bodies, and feature mounds and pits that are a result of multiple unsuccessful reprocessing attempts. During site investigations conducted in 2000 and 2014, standing water was observed in the pits within Ponds 2 and 4 (Dynamac Corporation 2010). Ponds 5–9 are relatively flat and show no evidence of the reprocessing related disturbances present in Ponds 1–4. Ponds 5–9 are composed of manganese oxide and carbonate dominated tailings derived from processing of manganese-oxide ores.

Hydrogeology

The Caselton Wash lies within the Great Basin Regional Aquifer System (Harrill et al. 1988). The Great Basin Regional Aquifer System contains three principal hydrogeologic units: basin-fill deposits, carbonate rocks, and volcanics. The basin-fill deposits are composed of unconsolidated silt, clay, gravel, and sand and commonly contain unconfined sub-basin aquifers. The carbonate rocks include massive consolidated Paleozoic strata, while the volcanic units consist mostly of tuffs and basalts of Tertiary age. Generally, the basin-fill deposits are located in intermontane valleys, overlying the volcanic formations, which overly the massive Paleozoic strata. The carbonate aquifers are typically confined systems with recharge originating as snow in high mountain range exposures and deep (> 300 m below ground surface) underflow. Basin fill aquifers are connected by varying degrees to the carbonate and volcanic aquifers via mountain front recharge, spring flows, and leakage between aquifers, and are internally drained by evaporative discharge, agricultural pumping, or drainage to underlying aquifers.

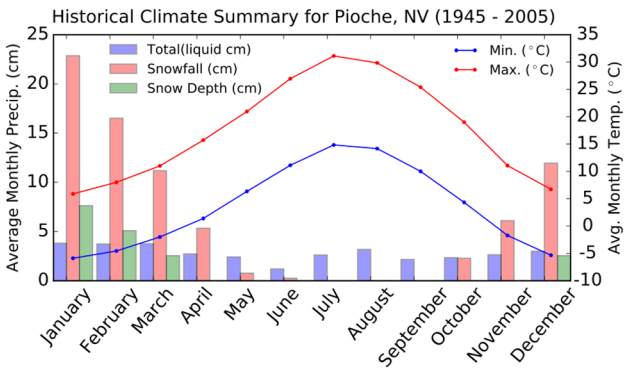

Fig. 2 Plot of monthly averaged daily minimum and maximum temperature and precipitation at Pioche, NV. Precipitation reported as total precipitation (liquid cm), snowfall (cm), and snow depth (cm)

The Caselton Wash tailings are located within a basin fill deposit near the northern boundary of the Panaca Valley Hydrographic Basin, which connects through Meadow Valley Wash to the Colorado River Basin (Fig. 1). Recent investigations have determined that basin fill below the tailings is at least 200 m thick, while the unconfined groundwater table is located ~ 100 m below the ground surface.

Field and Laboratory Data Collection and Hydrologic Parameter Development

Field Saturated Conductivity, In-situ Density, Moisture Content, and Dry Bulk Density

Field saturated hydraulic conductivity (K_{fs}) measurements were collected at two locations on Pond 4 using a METER (dba. Decagon Devices) DualHead Infiltrometer. The DualHead Infiltrometer uses a modified version of the Reynolds and Elrick (1990) method to estimate K_{fs}. In-situ tailings density measurements were collected at Pond 4 using the sand-cone (ASTM D1556) and drive-cylinder methods (ASTM 2937), resulting in tailings densities of 1.26 and 1.18 g/cm^3, respectively. Tailings samples were excavated using a trowel, and immediately sealed in plastic bags to prevent moisture loss. Moisture content and dry bulk density were determined in general accordance with ASTM D7263 and ASTM D2216.

Development of Water Retention Curves

Water retention curves (WRCs) for the tailings materials were developed using the hanging column method (ASTM D6836-Method A), the pressure plate method (ASTM D6836-Method B) and the chilled mirror hygrometer method (ASTM D6836-Method D). Equilibrium suction and moisture content data were fit to the van Genuchten–Mualem (vG-M) (1980), vG-M with a 2 cm air entry (Vogel et al.

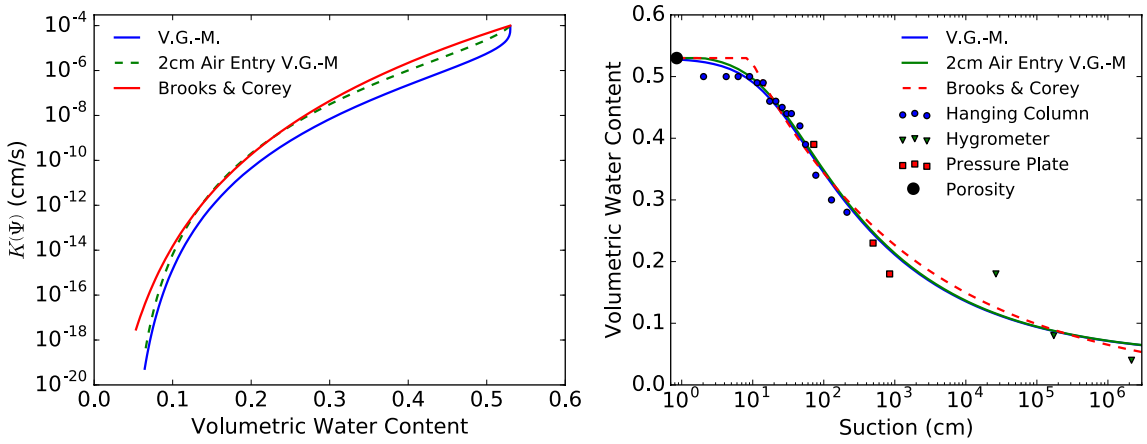

Fig. 3 H-K_ψ models and H-Ψ relationships regressed from measured equilibrium water content data using laboratory developed equilibrium outflow data. K_s is used as the base hydraulic conductivity for H-K_ψ models. Porosity determined by dry unit weight

Table 1 van Genuchten parameters for materials in Caselton simulations

Material	θ_r	θ_s	α (1/m)	n	K_s (cm/s)
Rosetta tailings	0.09	0.49	1.21	1.45	3.08×10^{-4}
Rosetta alluvium	0.04	0.34	1.33	1.44	1.29×10^{-4}
Loam	0.08	0.43	3.6	1.56	2.89×10^{-4}
Lab tailings, K_{fs}	0.04	0.53	5.75	1.26	1.52×10^{-3}
Lab tailings, K_s	0.04	0.53	5.75	1.26	1.00×10^{-4}
Lab tailings, K_{fs}, B.C.[1]	0	0.53	10.98	0.18	1.52×10^{-3}
Pre-existing HELP tailings	0.08	0.48	1.78	1.15	1.80×10^{-5}

Parameters are for the base case simulation, utilizing the Brooks and Corey (1964) hydraulic property model. Results for this model are plotted in Fig. 3

2000), and the Brooks and Corey (1964) hydraulic property models (Fig. 3). The vG-M (1980) model separately utilized K_{fs} and laboratory measured saturated hydraulic conductivity (K_s). Additionally, unsaturated hydraulic properties for Pond 4 tailings and alluvial soil were estimated using textural information from particle size distribution data and Rosetta Lite (Schaap 2003). Table 1 lists the vG-M parameters for materials used in simulations, while Fig. 4 shows the corresponding WRC and unsaturated hydraulic conductivity (K_ψ) function for each material.

Predictive Simulations of Caselton Tailings

Predictive simulations were conducted to estimate percolation through the Caselton Wash tailings to the underlying alluvium. A base case simulation was conducted with a numerical hydrologic model (HYDRUS 2D/3D). The base case simulation is intended to represent an optimal balance between model complexity and modeling feasibility, to best honor the available data, and represent defensible choices for numerical solution parameters (e.g. mesh discretization). Effects on percolation predictions of various, common

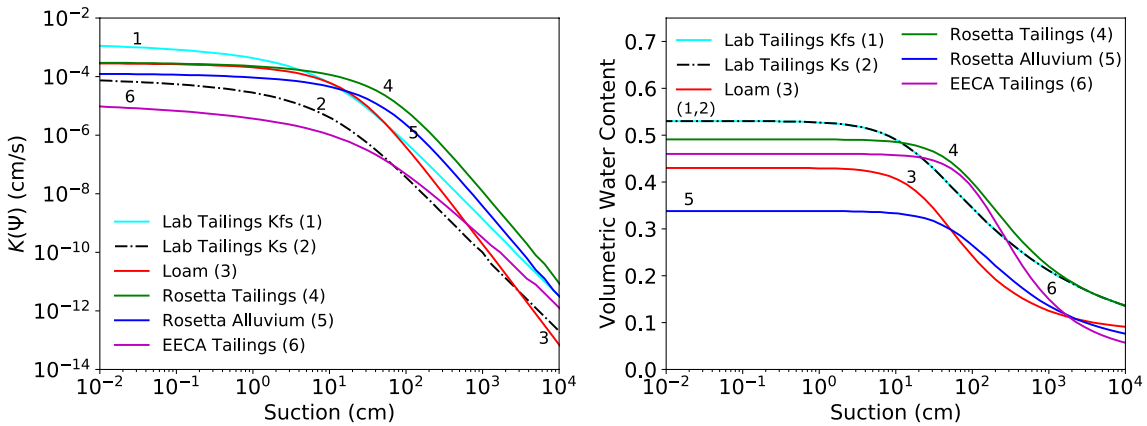

Fig. 4 H-K_ψ and H-Ψ relationships for materials used in simulations. Suctions are limited to 100 m. Parameters for curves are listed in Table 1

modeling decisions were analyzed by implementing changes in model parameterization and construction, one at a time. Additionally, an identically constructed simulation was conducted using the HELP model to investigate the effects of varying process simulation. A graphical summary of simulations conducted for this study (Fig. 5) shows the simulations arranged according to differences in parameterization and construction compared to the base case simulation.

Base Case Model

As shown in Fig. 5, the base-case model consists of a simulation conducted in HYDRUS 2D/3D with an approximated cross-sectional channel geometry, small finite element mesh (0.2 m global sizing, with 3.3 cm refinement at tailings surface), daily averaged boundary condition data calculated from a local MET station, hydraulic properties developed from laboratory measured equilibrium retention data and K_{fs}, a unit gradient lower boundary condition, and utilizes the vG-M (1980) hydraulic property model.

Initial Conditions

Initial conditions for all simulations were first specified to be in static equilibrium with a hypothetical water table located 10 m below the lowest model node. To accomplish static equilibrium, the pressure head was set equal to 0 m at the water table, and suction was increased jointly with elevation so that the initial suction at the surface was equal to the maximum model depth plus 10 m (Fig. 6). Models were subsequently executed with on-site climate data until steady state drainage rates were achieved. Final head distributions from the steady state models were then used as initial conditions for transient models. This procedure is standard practice for performing transient groundwater modeling (Anderson et al. 2015).

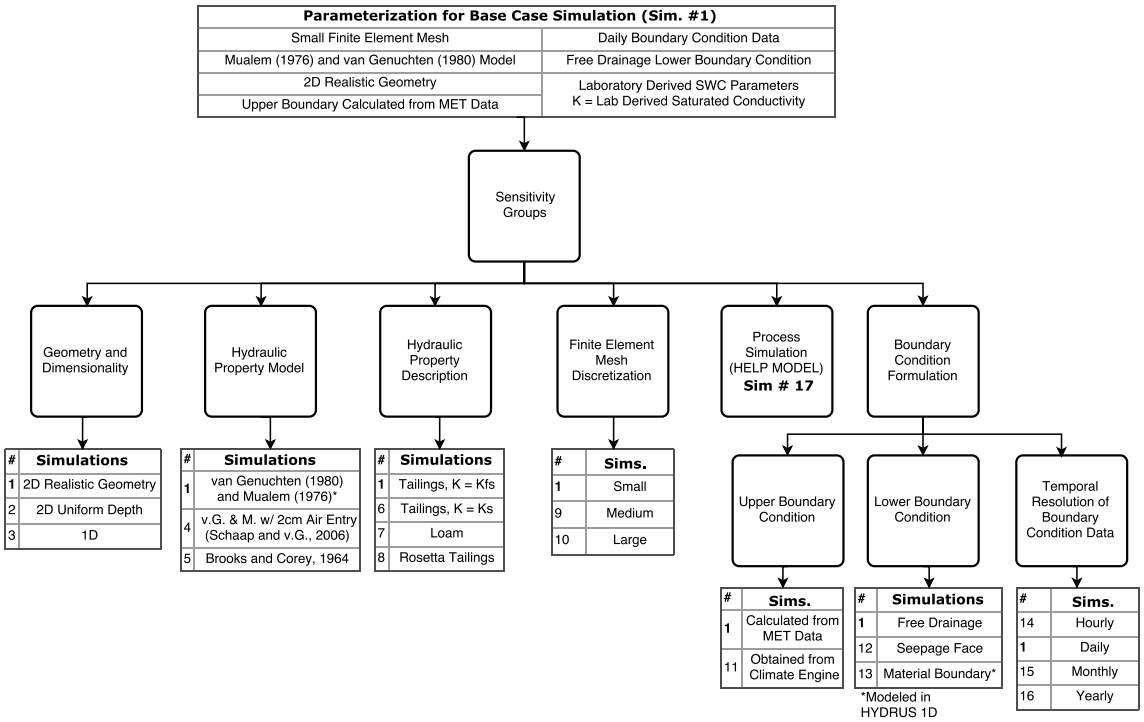

Fig. 5 Visual summary of simulations presented in this study. 1 represents the base case model in each group, while remaining numbers represent departures from the base case (remaining aspects are identical to the base case)

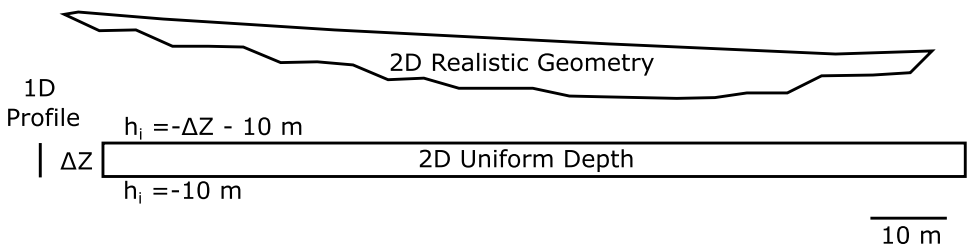

Fig. 6 Dimensionality and geometry types used in simulations

Model Dimensionality and Geometry

Figure 6 shows the types of domain geometries used in simulations for this study, which include 1D and 2D representations of the tailings. Realistic domain geometry was estimated from boring logs collected during previous remedial investigations (Dynamac Corporation 2010). The boring data was used in conjunction with land surface elevation data from the USGS National Elevation Dataset digital elevation model (DEM) (Gesch et al. 2002) to create upper and lower bounding surfaces for the tailings. Upper and lower bounding surfaces for the tailings were interpolated with a triangular irregular network (TIN) algorithm, after which their elevation was extracted along a 2D profile across Pond 4. Simplified geometries, which consisted of 1D and 2D uniform depth domains, assumed an average tailings depth of 4.6 m to be consistent with previous site models.

Hydraulic Property Model

Sensitivity to the hydraulic property model was examined by varying the hydraulic property model between the vG-M (1980) model, a version of the vG-M model modified with a 2 cm air entry pressure (Vogel et al. 2000), and the Brooks and Corey (1964) model. As shown in Fig. 3, the WRCs differ most in the air entry region, with the standard vG-M model having an air entry pressure of 0 cm, and the Brooks and Corey model having the greatest (≈ 10 cm for the tailings). The models also differ slightly in the middle to dry portions of the WRC in the shape of exponentially declining water content with suction.

Differences in the hydraulic property model significantly affect estimates of K_ψ throughout the saturation range. Figure 3 demonstrates that for the retention data used in this study, the Brooks and Corey model predicts the highest K_ψ values, while the vG-M model predicts the lowest K_ψ values. The 2 cm vG-M model retains the smooth shape of the retention curve from the vG-M model and predicts intermediate K_ψ values. Importantly, the rate at which K_ψ changes near saturation is much lower in the 2 cm vG-M model and Brooks and Corey models. As described by Vogel et al. (2000) and Schaap and van Genuchten (2006), the lower rate of change allows for a more accurate and less iterative numerical solution of Richards equation, as well as more accurate simulation of water retention properties for materials with significant air entry pressures.

Hydraulic Properties

The variety of hydraulic properties shown in Table 1 and Fig. 4 represent example parameterizations for an unsaturated numerical simulation. Hydraulic property descriptions include vG-M parameters corresponding to a loam from Rosetta (Carsel and Parrish 1988), tailings from Pond 4 developed from equilibrium water retention data that separately utilize K_{fs} and K_s, and tailings and alluvial material developed using textural information and Rosetta Lite (Schaap 2003). The inputs for the alluvial sample were 41.6% sand, 45.8% silt, and 12.6% clay by mass with a dry bulk density of 1.6 g/cm^3. The tailings inputs were 31% sand, 34.5% silt and clay with a dry bulk density of 1.22 g/cm^3.

Finite Element Discretization

Figure 7 shows the finite element discretizations used in simulations. Discretizations include a large mesh (3.7 m global), a medium mesh (0.6 m global with 0.2 m refinement at the atmospheric boundary), a small mesh (0.2 m global with 3.3 cm refinement at the atmospheric boundary), an hourly mesh (0.2 m global with a 1.5 cm refinement at the atmospheric boundary), and a mesh for the material boundary simulation (0.2 m global with 3.3 cm refinement at the atmospheric boundary, 2 cm refinement surrounding the lower boundary condition, and 0.25 m constant spacing to a depth of 100 m). To achieve the highest degree of equivalency, node locations for HYDRUS 1D models were extracted from HYDRUS 2D models along a vertical line. The node depths were then used to construct the HYDRUS 1D models. The hourly mesh was necessary for convergence of the model with hourly input data, and the effect of using the hourly mesh in simulations with daily input data was not analyzed. Mesh refinements were placed in areas where steep, non-linear hydraulic gradients were expected to occur (Fig. 7). Such steep gradients occur most commonly at the atmospheric boundary but can also occur in transient simulations near material boundaries, wetting fronts, and lower boundary conditions.

Boundary Conditions

Upper Boundary Conditions

Upper boundaries were represented with an atmospheric boundary condition for all simulations. Inputs to atmospheric boundary conditions consist of precipitation and potential evapotranspiration (PET). To assess variability from differing atmospheric boundary condition calculation procedures, PET was calculated from a meteorological (MET) station in Pioche, NV (5 km NE of the site), or gathered from the Climate Engine web application (Huntington et al. 2017). In addition, hourly PET and precipitation from the MET station was averaged to daily, monthly, and yearly intervals to investigate effects on percolation predictions. The MET station is managed by the Community Environmental Monitoring Program (CEMP 2016), while records

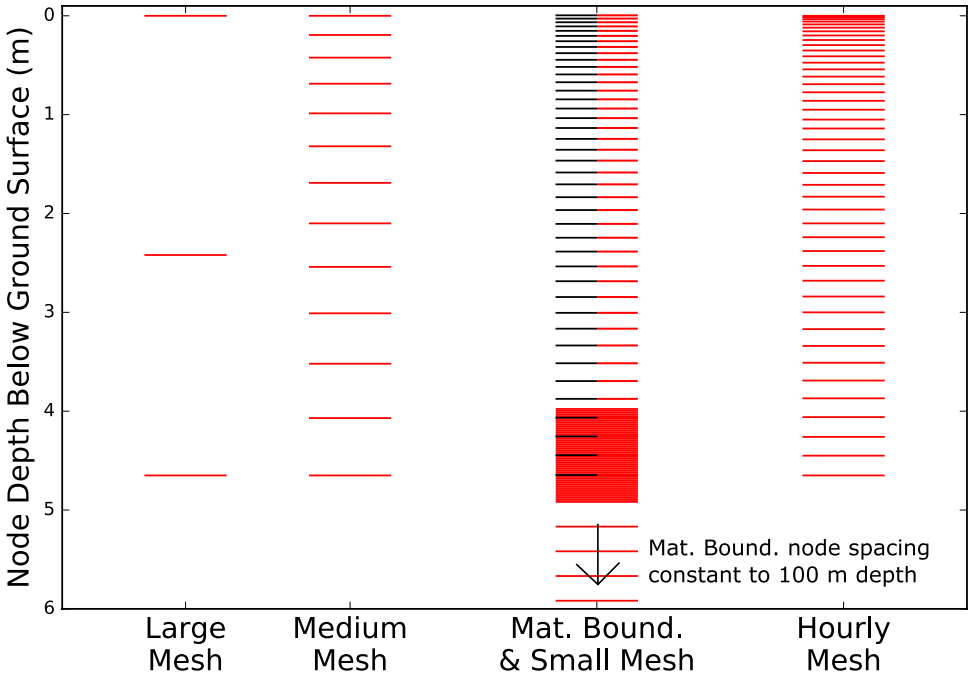

Fig. 7 Finite element discretization for all simulations. The small (black lines) and 1D material boundary meshes are identical aside from increased discretization near the tailings/alluvium boundary

from Climate Engine were selected from the gridMET/METDATA dataset (Abatzoglou 2013). Although daily climate records from the Climate Engine application are available from 1974 to present, the data used were from over a period consistent with the data coverage of the MET station, August 1998 to December 2014.

Owing to the paucity of vegetation on the tailings surface, the potential evaporation was calculated from MET data with the Penman (1948) equation for evaporation from an open water source. Soil heat flux was estimated as 10% of net radiation during the daylight hours, and 50% of net radiation during night time hours, while incoming extraterrestrial shortwave radiation was calculated using celestial geometry and site location information (Allen et al. 1998). Hourly records of air temperature, relative humidity, and wind speed were obtained from the MET station, while ground level incoming short wave radiation values were obtained from the National Renewable Energy Laboratory National Solar Radiation Database (2016) as global horizontal irradiance. Precipitation records were used directly from the MET station and Climate Engine datasets.

Lower Boundary Conditions

Several lower boundary conditions that could describe the tailings alluvium boundary in the absence of monitoring data were implemented to examine their effect on predicted percolation. As detailed in Fig. 5, lower boundary conditions included unit gradient, seepage face, and material boundary representations.

A unit gradient boundary condition simulates a scenario where matric and osmotic gradients are negligible and gravitational potential energy is the major contributor to the (vertical) hydraulic gradient. Although no suction measurements near the tailings/alluvium boundary were available, observational studies conducted in similar climates suggest that a unit hydraulic gradient may exist as near as 20 cm to the surface (McCord 1991; McCord et al. 1991; Sisson 1987).

The material boundary was represented by including a layer of alluvium beneath the tailings. The hydraulic properties for the alluvium are listed in Table 1. The lower boundary condition for the alluvium was set to be a constant head value of 0 m (saturated) at 100 m below ground surface. Simulation was conducted with HYDRUS 1D for computational efficiency, as a 2D domain with appropriate discretization for this simulation would be prohibitively large.

Seepage face boundary conditions simulate a scenario where the porous media is exposed to an air interface, with fluid seeping from the porous media. Fluid flow across the boundary occurs when total head is greater than 0 (or another user-specified value). Scanlon et al. (2002) showed that seepage face boundary conditions can be approximated by placing a coarsely textured material (e.g. gravel) underneath a fine-grained material. The material boundary between the fine-grained tailings and the relatively coarse-grained alluvium could conceivably behave as a seepage face boundary in this fashion.

Process Simulation

A simulation utilizing the (1D) HELP model was constructed using boundary conditions and hydraulic properties identical to the base case simulation. Hydraulic property model and mesh discretization do not apply to the HELP model, as it does not numerically solve Richards equation. The Dynamac Corporation (2010) HELP simulation was also included to illustrate the combined effects of variations in modeling practice and the non-uniqueness of unsaturated water balance calculations. Hydraulic properties for this simulation are shown in Table 1.

The principal difference between HELP and HYDRUS is that HYDRUS numerically solves Richards equation, while HELP uses a water routing and storage method. Differences in percolation are driven primarily by the process simulation for flow within and removal of water by evapotranspiration from a porous media. In arid climates, removal of water by evapotranspiration can represent a significant portion of the water balance (Scanlon et al. 2005). In HYDRUS and other Richards equation-based models, PET drives upward matric gradients, resulting in flux of water to the atmospheric boundary. In the HELP model, water removal by evapotranspiration is simulated with a sink term from an evaporative zone when the water content is above the wilting point. The evaporative zone extends from the surface to a depth that is based on site location, soil, and vegetation parameters.

For flow within porous media, the significant difference is that HYDRUS uses Richards equation, simulating matric gradients with a variety of boundary conditions to compute fluxes, while HELP assumes that a gravity drainage gradient (i.e. a downward gradient of one) exists throughout the domain. Khire et al. (1997) documented that the HELP model significantly over-predicted percolation, while another Richards equation-based model slightly under-predicted percolation. Scanlon et al. (2002) reached similar conclusions regarding the over-prediction of percolation by HELP compared Richards equation-based models. An issue related to process simulation and model selection not explicitly considered in this study is variability in conceptual model and modeler bias. These factors have the potential to contribute significant variability to model outputs. Modeling approaches that consider multiple scenarios are more likely to fully bracket the range of possible outputs and address the concerns of all stakeholders (Ferré et al. 2017).

Results/Discussion

Base Case Results

The base case simulation predicted two significant (~ 0.2 m) infiltration events; one from September 2004 to May 2005, and one from December 2010 to April 2011 (Fig. 8). The infiltration events were predicted during periods of sustained precipitation and low PET. Initially, infiltration is partitioned to water storage. Subsequently, stored water is partitioned to evaporative flux and drainage. In the base case, and for all models, insignificant amounts of runoff were predicted.

Evaporative conditions prevail at the Site at all temporal resolutions (Fig. 9). However, evaporative flux is severely limited when the tailings are dry near the surface. During evaporation, K_ψ at the atmospheric boundary decreases as the tailings dry out. Despite large upward gradients, evaporation is limited by low K_ψ, approaching zero within days - weeks of rainfall depending on the moisture state of the tailings and subsequent weather patterns. This behavior can be seen in the model results in Fig. 8 and has been demonstrated in the literature (Shah et al. 2007).

In contrast to evaporation, K_ψ increases at the atmospheric boundary as water flows into the tailings during infiltration. Increased K_ψ, along with gravity and matric gradients, drive large amounts of infiltration over short periods of time compared to evaporation. Infiltrative head gradients can be initially steep, but typically decline as the infiltration front advances into wetter media at depth. Infiltration and evaporation dynamics drive much of the system behavior, and accurate simulation requires careful consideration of

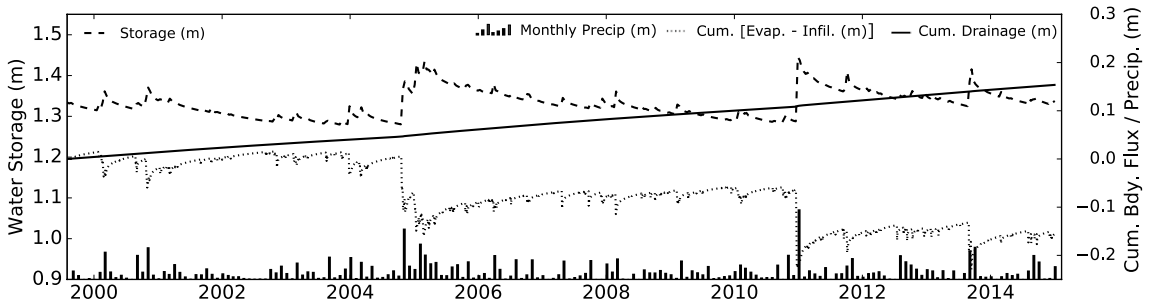

Fig. 8 Results for the base case simulation. Infiltration events are driven by winter precipitation when PET is low. Evaporation occurs over longer time scales than infiltration. Drainage rates are relatively constant over time. Monthly precipitation is scaled with the secondary y axis, and zero-referenced at the minimum secondary y axis value

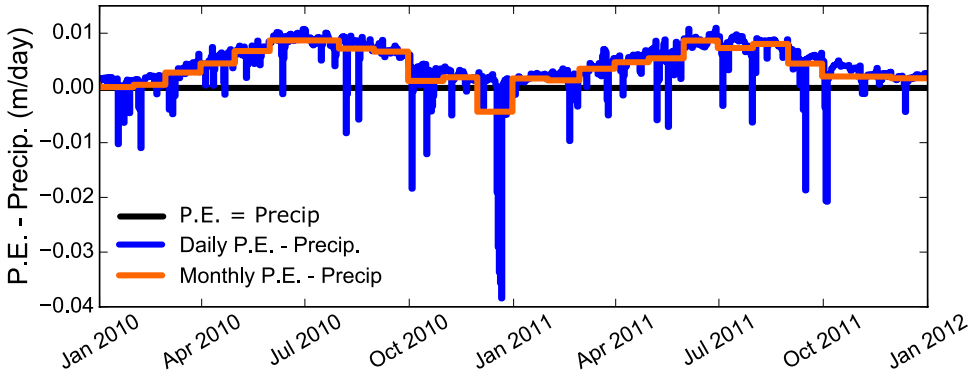

Fig. 9 Potential evaporation minus precipitation rate at daily and monthly resolutions. Precipitation rate exceeds potential evaporation rate more frequently at smaller temporal resolutions, leading to more infiltration

associated modeling decisions (e.g. mesh discretization, temporal resolution of boundary condition data).

Figure 8 shows that the base case model predicted 0.15 m of cumulative drainage, -0.15 m of net infiltration, and 1.35 m of water storage over the 15.4-year simulation. The steady state drainage rate for the base case simulation was 9.5 mm/year. (Table 2; Fig. 10), or about 4% of the average annual precipitation (0.23 m).

Sensitivity to the Hydraulic Property Model

Figure 11f shows that compared to the base case, net evaporation was greater by 0.08 m in the Brooks and Corey model and 0.06 m in the 2 cm vG-M model, while drainage was decreased by the same amount for each model, and water storage was decreased by 0.25 m and 0.2 m, respectively. Most of the difference in surface flux between hydraulic property models is due to evaporation dynamics (Fig. 12). In contrast, infiltration events behaved nearly identically, regardless of hydraulic property models. The differences between the hydraulic property models are most likely due to higher predicted K_ψ at dry states relative to the vG-M model (Fig. 3). Higher predicted K_ψ at dry states drives increased evaporative flux, depleting water storage and limiting drainage. Varying the hydraulic property model affected steady state drainage rates by 0.005 m/year. or a 50.2% decrease with respect to the base case simulation (Table 2; Fig. 10).

Table 2 Steady state results for Caselton models

Model number	Steady state drainage rate (m/year)	% increase from base case (%)	Min. Δt (s)	Cumulative mass balance error (%)[a]	Sensitivity parameter
1	9.54×10^{-3}	0.0	8.6×10^{-3}	0.064	Base case
2	1.01×10^{-2}	5.3	8.6×10^{-1}	0.097	2D uniform depth
3	8.5×10^{-3}	− 10.9	8.6×10^{-4}	0.011	1D
4	6.28×10^{-3}	− 34.2	8.6×10^{-3}	0.008	2 cm vG-M
5	4.75×10^{-3}	− 50.2	8.6×10^{-3}	0.005	Brooks and Corey
6	1.90×10^{-2}	99.2	8.6×10^{-3}	0.135	Ks tailings
7	2.36×10^{-2}	147.4	8.6×10^{-3}	0.161	Loam
8	6.01×10^{-3}	− 37.0	8.6×10^{-3}	0.015	Rosetta tailings
9	3.18×10^{-3}	− 66.7	8.6×10^{-4}	1.341	Medium mesh
10	1.25×10^{-4}	− 98.7	8.6×10^{-4}	1.58	Large mesh
11	1.56×10^{-2}	63.7	8.6×10^{-3}	0.128	Climate engine
12	6.68×10^{-3}	− 29.9	8.6×10^{-3}	0.044	Seepage face
13	8.96×10^{-3}	− 6.1	8.6×10^{-4}	0.047	Material boundary
14	1.48×10^{-2}	55.2	3.6×10^{-9}	3.12	Hourly
15	9.81×10^{-4}	− 89.7	2.8×10^{-5}	0.397	Monthly
16	0	− 100.0	8.6×10^{-4}	0.473	Yearly
17	5.1×10^{-2}	434.6	N/A	N/A	HELP
18	3.2×10^{-3}	− 66.5	N/A	N/A	Pre-existing HELP

Distinguishing features for each model can be identified by sensitivity parameter or by model number with Fig. 5

[a]Over the 15.4 year simulation period

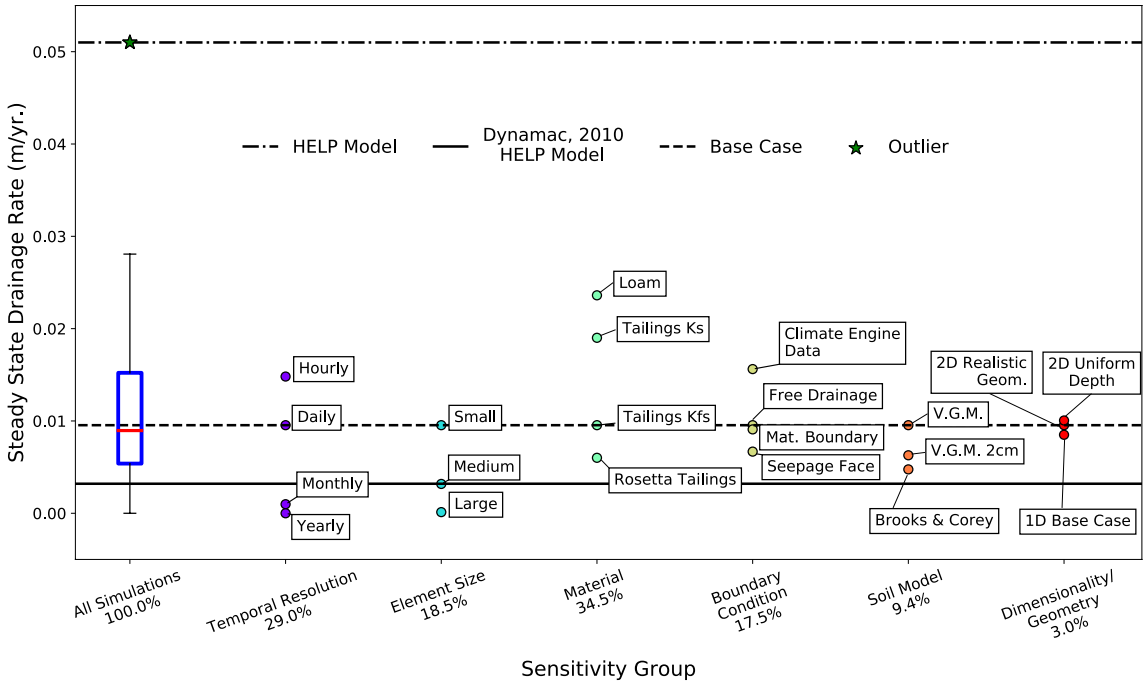

Fig. 10 Steady state drainage rates for all models by sensitivity group. Percent of total variation for each sensitivity group is shown on the x axis

Sensitivity to Hydraulic Properties

Similar to the hydraulic property model, evaporation dynamics drive a significant portion of variability in percolation due to varying hydraulic property description. Variability in K_ψ at dry states drives variability in evaporation, affecting the amount of water storage available for drainage. During evaporative periods, the upper boundary condition is limited to 100 m (10^4 cm) suction to prevent instability in the numerical solution. At 10^4 cm suction, K_ψ for the Loam, K_s based tailings are 2–3 orders of magnitude less than those for the K_{fs} based tailings and Rosetta tailings (Fig. 4), limiting upward fluxes toward the atmospheric boundary. Although K_s differs between the materials (Fig. 4; Table 1), saturation is rarely achieved and precipitation rates infrequently exceed K_s for any of the materials, limiting differences in infiltration due to K_ψ near saturation.

Figure 11e shows that the Loam and Ks tailings property descriptions (Table 1) result in less evaporation (and subsequently, more drainage) compared to the K_{fs} and Rosetta based tailings. Changes in water storage were related to differences in the hydraulic capacity of each material (Fig. 4), as well differences in drainage, infiltration, and evaporation from the K_ψ effects discussed previously. Predicted drainage was reduced by 0.06 m for the Rosetta model and increased by 0.14 m and 0.2 m for the K_s and loam based hydraulic property descriptions, respectively (Fig. 11e). Net evaporation was increased by 0.21 m and 0.15 m for the loam and K_s based property descriptions, while it increased by 0.06 m for the Rosetta description. Storage was increased by 0.43 m for the K_s based description and reduced by 0.36 m and 0.23 m for the loam and Rosetta descriptions. Differences in material properties affected steady state drainage rates by 0.014 m/year, or a 147.4% increase with respect to the base case simulation (Table 2; Fig. 10).

Sensitivity to Finite Element Discretization

Increasing element size resulted in lower predicted infiltration, as well as higher predicted evaporation (Fig. 13). Relative to the base case, drainage was decreased by 0.15 m and 0.09 m for the large and medium discretization, respectively (Fig. 11a). Net evaporation was increased by 0.3 m in the large discretization and 0.15 m in the medium discretization. Storage was lower by 0.55 m and 0.11 m in the large and medium discretization, respectively. In addition, mass balance errors were higher for the large and medium discretizations compared to the base case (Table 2). Steady state drainage rates were decreased by 0.009 m/year for the large element simulation, or a 98.7% decrease with respect to the base case simulation (Table 2; Fig. 10).

The differences between the simulations are related to the ability of linear finite elements to accurately simulate steep, non-linear head gradients near the surface. This occurs most commonly during late stage evaporation, as described by Hayhoe (1978), but can occur with any steep head gradients (e.g. infiltration fronts). Figure 14 illustrates this concept by contrasting final head distributions for the small, medium,

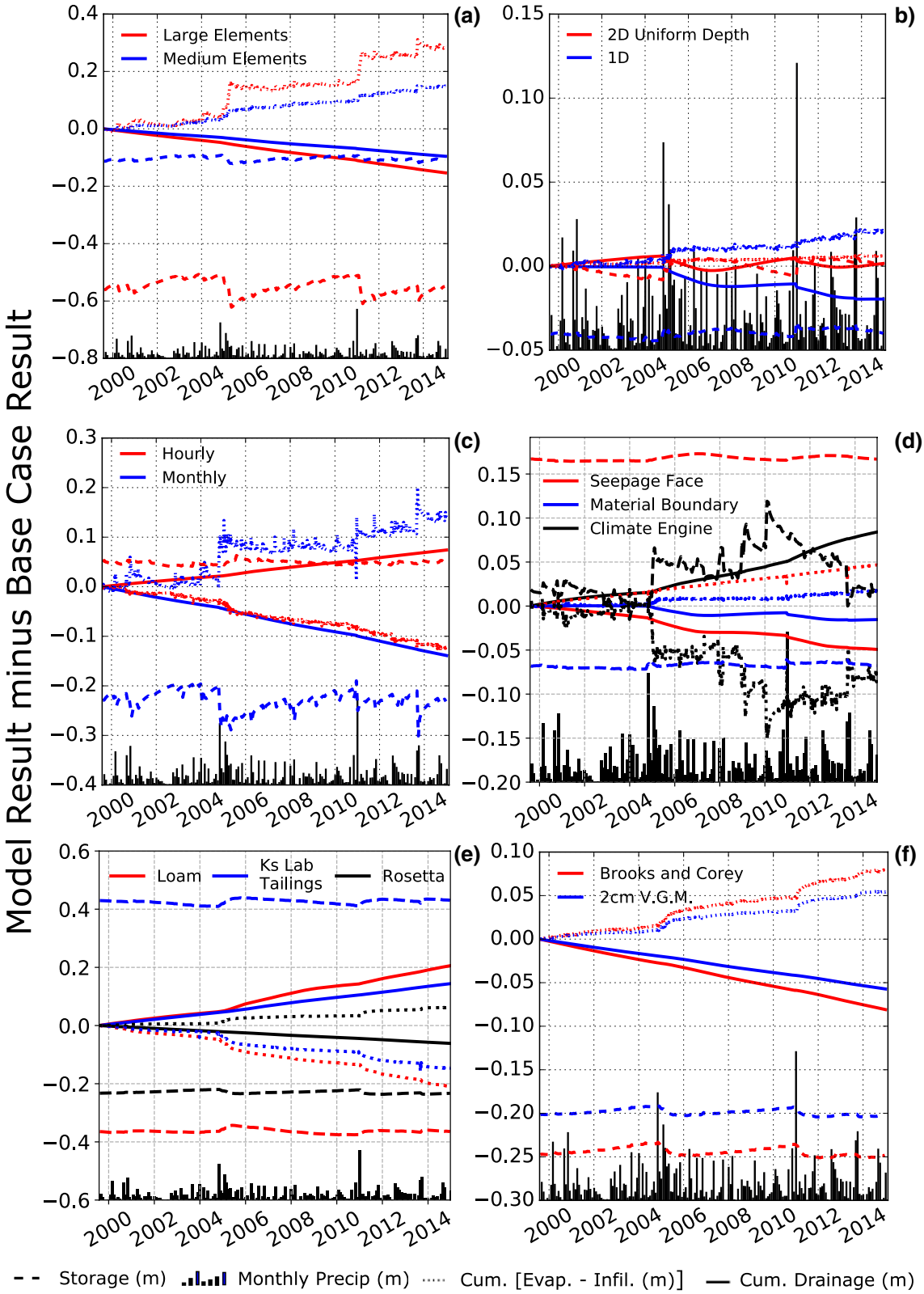

Fig. 11 Transient results for all simulations, reported as a difference from the base case. Base case results would plot as 0 for cumulative drainage (solid line), cumulative atmospheric flux (dotted line), and water storage (dashed dotted line). Monthly precipitation totals are scaled with individual y-axes, and zero-referenced at the y axis minimum

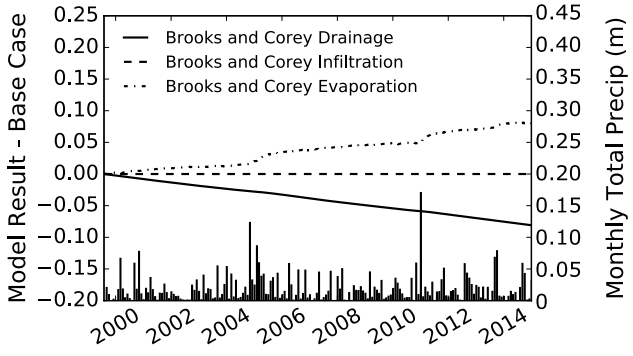

Fig. 12 Surface fluxes, separated as infiltration and evaporation, for Brooks and Corey hydraulic property model differenced from the base case. Infiltration is indistinguishable, while evaporation is greater in the Brooks and Corey model due to increased K_ψ in drier conditions. The 2 cm vG-M model behaved similarly to the Brooks and Corey model

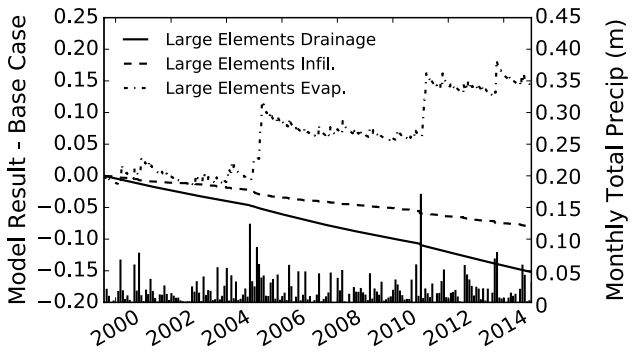

Fig. 13 Surface fluxes, separated as infiltration and evaporation, for varying finite element discretization differenced from the base case. For larger element sizes, mis-representation of system behavior due to coarse discretization (see Fig. 14) leads to increases in evaporation and decreases in infiltration, resulting in less drainage

and large finite element meshes. The steep increases in suction, and transition to unit gradient conditions near the surface displayed in the small discretization is consistent with observational studies (McCord 1991; McCord et al. 1991; Sisson 1987), while the large discretization unrealistically extends suctions along a linear gradient to depths of several meters. The effect of such erroneous (for bare tailings) suctions at depth is conveyance of water to the surface. This effect was especially pronounced following infiltration events from September 2004 to May 2005 and December 2010 to April 2011 (Fig. 11a).

Evaporative flux is less in the smaller discretization due to the sharp suction gradient near the surface (Fig. 14) and corresponding decreases in K_ψ, which have a flux limiting effect. In addition, unit gradient head distributions at depth in the small and medium mesh allow water to gravity drain, while the linear suction gradient in the large discretization

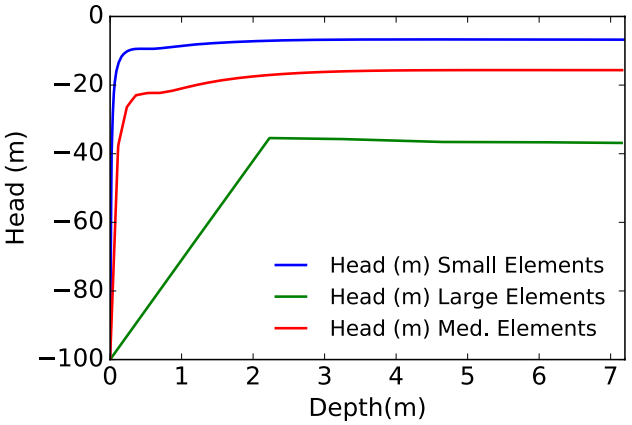

Fig. 14 Vertical profile of final head distributions for varying element size

drives flux from depth towards the surface. Variability in predicted infiltration due to changes in discretization is relatively less because infiltration occurs over shorter timescales, and with more linear head gradients than evaporation. Differences in predicted water storage due to discretization are related to simulation of infiltration and evaporation rather than the ability to simulate water storage. The large and medium discretizations are not adequately refined near the surface and are included here for demonstration. Proper finite element sizing at the upper boundary is closely related to the length scales of evaporation and infiltration, which are 1–6 cm (Lehmann et al. 2008; Šimunek and; Miroslav 2009; White and Sully 1987).

Sensitivity to Boundary Conditions

Sensitivity to Upper Boundary Conditions

Models executed with upper boundary condition data gathered from Climate Engine predicted 0.08 m more drainage than models using a combination of MET data from nearby Pioche, NV and remotely sensed radiation values, due to increased precipitation in the Climate Engine dataset (Fig. 11d). Increased precipitation in the Climate Engine dataset led to 0.08 m more net infiltration and 0.02 m more water storage compared to the base case. Positive biases for gridMET precipitation data relative to individual MET station data in the great basin are reported by Abatzoglou (2013) and Breitmeyer et al. (2018), where they are attributed to gauge under-catch, especially of solid phase precipitation on automated gauges that are not winterized, as detailed by Legates and DeLiberty (1993). Use of the gridMET upper boundary condition data increased steady state drainage rates by 0.006 m/year, or by 63.7% with respect to the base case simulation (Table 2; Fig. 10).

Sensitivity to Temporal Resolution of Boundary Condition Data

Infiltration events occur when the precipitation rate exceeds the actual evaporation rate. Averaging of climate forcing data over larger time periods in the daily (base case) and monthly simulations resulted in fewer instances of precipitation rate exceeding potential evaporation (Fig. 9), with yearly averages always being net evaporative. Compared to the base case simulation using daily averaged climate data, the hourly simulation resulted in an increase in drainage of 0.07 m, while the monthly simulation resulted in a decrease of 0.14 m. The hourly simulation predicted an increase of 0.13 m in net infiltration, while the monthly simulation predicted a decrease of 0.14 m in net infiltration. Storage was higher by 0.05 m in the hourly simulation and lower by 0.23 m in the monthly simulation (Fig. 11c). The hourly steady state drainage rate was greater than the base case drainage rate by 0.005 m/year or a 55.2% increase, while the monthly model was less than the base case rate by 0.009 m/year an 89.7% decrease (Table 2; Fig. 10). Mass balance errors for the hourly simulation were the highest of all simulations, at 3.12%. Drainage rates for the yearly averaged boundary condition data decline exponentially and approach zero drainage. Yearly averaged boundary condition data are not considered physically realistic and are not plotted on Fig. 11c.

Sensitivity to Lower Boundary Conditions

Figure 11d shows that water storage was greater than the base case by 0.17 m in the seepage face simulation and less than the base case by 0.07 m in the material boundary simulation. Water storage in the seepage face model is higher than the base case because positive pore pressure is requisite for drainage through a seepage face boundary condition. Varying the lower boundary condition resulted in a 0.01 m decrease in drainage of for the material boundary, and a 0.05 m decrease for the seepage face boundary compared to the base case free drainage simulation. Net evaporation was greater than base case by 0.05 m and 0.01 m in the seepage face and material boundary models, respectively. The increase in net evaporation for the seepage face model is due to higher saturation and K_ψ near the atmospheric boundary. Increased evaporation and decreased storage in the material boundary simulation is likely related to differences in simulation of evaporation in HYDRUS 1D for the material boundary compared to HYDRUS 2D for the base case and is discussed in the dimensionality and geometry section. Variation in choice of lower boundary condition increased steady state drainage rates by 0.006 m/year, or a 63.7% increase with respect to the base case simulation (Table 2; Fig. 10).

Sensitivity to Model Dimensionality and Geometry

Simplified geometries consisted of 1D and 2D uniform depth domains and assumed an average tailings depth of 4.6 m for consistency with previous models (Fig. 6). To provide consistency across varying geometry and dimensionality, water storage for the simplified geometries were normalized to the average depth of the 2D realistic channel geometry (4.9 m).

Differences in model predictions due to model dimensionality and geometry are relatively small compared to effects from other factors (Figs. 10, 11), suggesting that dimensionality and geometry effects may be insignificant as long as results are normalized to achieve direct comparison. Figure 15 shows that the 1D model predicted less drainage than the 2D models over the simulation period, due to more predicted evaporation in the 1D model. The larger difference in predicted drainage for the 1D simulation compared to the 2D uniform depth simulation suggests that dimensionality has a more measurable effect than geometry. However, the differences between the 1D and 2D simulations is also related to the difficulty of achieving equivalent discretization in 1D and 2D finite element models and differences in solution technique between HYDRUS 1D and 2D, both of which contribute to variability in model output.

Depth-averaging of complicated geometries has the potential to misrepresent depth-dependent processes. For instance, in deeper portions of the domain, increased storage capacity allows stored water to evaporate between precipitation events. In shallow portions, stored water is lost via the lower boundary more quickly. Depth dependency becomes less important when the lower boundary is represented by a material boundary, as water can enter and exit material boundaries according to time-varying head distributions.

While constructing completely identical simulations in 1D and 2D models presents challenges for the practitioner, the relatively minor differences in drainage due to varying

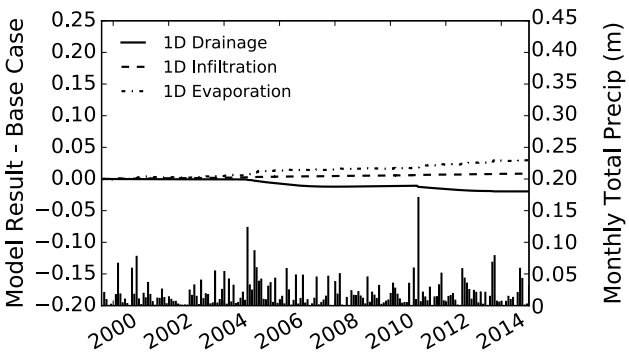

Fig. 15 Surface fluxes, separated as infiltration and evaporation, for varying dimensionality and geometry differenced from the base case. Differences in evaporation are larger than infiltration. The effects of dimensionality and geometry are relatively minor compared to other effects

dimensionality for simulations in this study suggest that other factors can more significantly affect drainage estimates. More significant differences due to dimensionality are expected for mine waste materials with significant exposure above the ground surface (e.g. heap leach pads, waste rock piles). Above ground mine waste materials can experience chemical and hydraulic effects related to aspect, geometry dependent radiation and wind exposure, and may require explicit consideration of the air phase (Amos et al. 2009).

As shown in Fig. 10, drainage in the 1D model was 0.02 m less than the base case model, compared to an increase of 0.002 m in the 2D uniform depth model. Net evaporation was 0.02 m greater than base case in the 1D model, and 0.006 m greater in the uniform depth 2D model. Storage was less than the base case by 0.04 m and 0.001 m for the 1D and 2D uniform depth models, respectively. 1D steady state drainage was less than the 2D base case by 0.001 m/year, a 10.9% decrease with respect to the base case simulation, while the 2D uniform depth simulation predicted an increase of 0.0006 m/year, or an increase of 5.34% (Table 2; Fig. 10).

Process Simulation

Steady state drainage rates from a pre-existing HELP model reported by Dynamac Corporation (2010) were less than the 2D base case model by 0.006 m/year, a 66.5% decrease while the HELP model constructed comparably to the base case was greater than the base case by 0.041 m/year, a 434.6% increase (Table 2; Fig. 10). The relative agreement of the pre-existing HELP model is surprising, considering the significant differences in hydraulic properties between the HELP simulation and laboratory derived properties (Table 1; Fig. 4), the simplification of governing processes in the HELP model (e.g. no simulation of matric gradients), and the use of data from a stochastic weather generating routine compared to locally gathered climate data. However, due to the non-unique nature of unsaturated hydrologic models, many different combinations of model parameters and modeling assumptions can arrive at similar solutions. The non-unique nature of unsaturated hydrologic models implicates the need for experimental validation of as many measurable model parameters, boundary conditions, and outputs as possible, and the verification that parameters related to the numerical solution (e.g. element sizing) are chosen appropriately.

Model execution times for a HYDRUS 1D and HELP simulation range from seconds to minutes, meaning similar types of stochastic sensitivity analysis could feasibly be conducted on both models. However, construction of a Richards Equation-based simulation (e.g. HYDRUS 1D) takes considerably more modeling skill and understanding of numerical solution parameters and unsaturated flow processes, in addition to sometimes requiring costly and time-consuming development of unsaturated soil parameters. In contrast, HELP was designed for barrier style cover and liner systems, and most user interfaces have streamlined model construction for these types of systems. When a conservative, first order assessment of water balance is needed, especially in a humid climate, simplified models such as HELP may be a practical choice. However, when dynamic system behaviors are required for more detailed analysis, such as fate and transport assessments or when evapotranspiration is the main mechanism for preventing percolation, a more process-based model such as HYRDRUS 1D is required (Berger 2000).

Conclusions

Predictive modeling of percolation through the Caselton Wash tailings conducted under a range of assumptions, parameterization methods, and modeling practices predicted steady state drainage rates of 0–51 mm/year. The variability in drainage predictions is noteworthy, as most parameterizations are defensible approaches considering the paucity of data for this site. This study highlights the importance of model parameterization techniques, appropriate selection of boundary conditions and spatial discretization, and verification of model predictions with monitoring data. The main findings from this study were:

1. Numerical hydrologic models were most sensitive to choice of hydraulic properties, accounting for 34.5% of the total variability in steady state drainage rate (0–24 mm). Temporal resolution of boundary conditions, element size, and choice of upper and lower boundary condition also contributed significant variability (29.0%, 18.5%, and 17.5%, respectively).
2. Choice of the hydraulic property model and dimensionality and geometry contributed 9.4% and 3.0% of total variability but may have significant impacts on convergence and runtime. Translating results between differing geometry and dimensionality requires careful normalization. The large and medium discretizations and monthly and yearly averaged boundary condition data were included for demonstration and are not considered reasonable modeling choices for site scale percolation prediction.
3. Variations in process simulation, as represented in this study using a simplified model (HELP) and a mechanistic model (HYDRUS), introduced more variability in predicted percolation than any of the modeling choices in the mechanistic model. In arid climates, simplified models like HELP are expected to over-predict drainage due to under-predicting evaporation. A HELP simulation

parameterized identically to the base case predicted a 434% increase in drainage relative to the base case.

4. Hydraulic properties should be measured as accurately as possible with repacked or in-situ laboratory specimens, or through numerical inversion of transient monitoring data. When feasible, boundary condition choices should be supported by on-site meteorological and monitoring data. In the absence of on-site boundary condition data, a range of potential boundary conditions can be used to bracket upper and lower bounds on drainage predictions.

Acknowledgements Financial and logistical support for portions of this study were provided by the Greenfield Environmental Multistate Trust, LLC—Trustee of the Multistate Environmental Response Trust, the Nevada Mining Association, Brown and Caldwell, Broadbent and Associates, and the Nevada Division of Environmental Protection, Abandoned Mine Lands Branch.

References

Abatzoglou JT (2013) Development of gridded surface meteorological data for ecological applications and modelling. Int J Climatol 33:121–131

Allen RG, Pereira LS, Raes D, Martin S (1998) Crop evapotranspiration-guidelines for computing crop water requirements-FAO irrigation and drainage paper 56. FAO Rome 300:D05109

Amos RT, Blowes DW, Smith L, Sego DC (2009) Measurement of wind-induced pressure gradients in a waste rock pile. Vadose Zone J 8:953–962

Anderson MP, Woessner WW (1992) Applied groundwater modeling: simulation of flow and advective transport. Academic Press, New York

ASTM D 1556 (2015) Standard test method for density and unit weight of soil in place by sand-cone method. In: Annual book of ASTM standards. ASTM International, West Conshohocken

ASTM D 2216 (2010) Standard test methods for laboratory determination of water (moisture) content of soil and rock by mass. In: Annual book of ASTM standards. ASTM International, West Conshohocken

ASTM D 2937 (2010) Standard test method for density of soil in place by the drive-cylinder method. In: Annual book of ASTM standards. ASTM International, West Conshohocken

ASTM D 6836 (2008) standard test methods for determination of the soil water characteristic curve for desorption using hanging column, pressure extractor, chilled mirror hygrometer, or centrifuge. In: Annual book of ASTM standards. ASTM International, West Conshohocken

ASTM D 7263 (2009) Standard test methods for laboratory determination of density (unit weight) of soil specimens. In: Annual book of ASTM standards. ASTM International, West Conshohocken

Berger K (2000) Validation of the hydrologic evaluation of landfill performance (HELP) model for simulating the water balance of cover systems. Environ Geol 39:1261–1274

Breitmeyer RJ, Stewart MK, Huntington JL (2018) Evaluation of gridded meteorological data for calculating water balance cover storage requirements. Vadose Zone J 17 (1). https://doi.org/10.2136/vzj2018.01.0009

Brooks RH, Corey AT (1964) Hydraulic properties of porous media and their relation to drainage design. Trans ASAE 7:0026–0028

Carsel RF, Parrish RS (1988) Developing joint probability distributions of soil water retention characteristics. Water Resour Res 24:755–769

Community Environmental Monitoring Program (2016) http://www.cemp.dri.edu/cgi-bin/cemp_stations.pl?stn=pioc. Accessed 1 March 2016

Dynamac Corporation (2010) Engineering evaluation/cost analysis—caselton tailings Site Lincoln County, Nevada. U.S. Army Corp of Engineers, Albuquerque District

Gesch D, Oimoen M, Greenlee S, Nelson C, Steuck M, Tyler D (2002) The national elevation dataset. Photogramm Eng Rem S 68(1):5–32

Harrill JR, Gates JS, Thomas JM (1988) Major ground-water flow systems in the Great Basin region of Nevada, Utah, and adjacent states

Hayhoe HN (1978) Study of the relative efficiency of finite difference and Galerkin techniques for modeling soil-water transfer. Water Resour Res 14:97–102

Huntington JL, Hegewisch KC, Daudert B, Morton CG, Abatzoglou JT, McEvoy DJ, Tyler E (2017) Climate engine: cloud computing and visualization of climate and remote sensing data for advanced natural resource monitoring and process understanding. Bull Am Meteorol Soc 98:2397–2410

Jung MC (2001) Heavy metal contamination of soils and waters in and around the Imcheon Au–Ag mine, Korea. Appl Geochem 16:1369–1375

Khire M, Benson C, Bosscher P (1997) Water balance modeling of earthen final covers. J Geotech Geoenviron 123:744–754

Legates DR, DeLiberty TL (1993) Precipitation measurement biases in the United States. J Am Water Resour Assoc 29:855–861

Lehmann P, Assouline S, Or D (2008) Characteristic lengths affecting evaporative drying of porous media. Phys Rev E 77(5):056309

McCord JT (1991) Application of second-type boundaries in unsaturated flow modeling. Water Resour Res 27:3257–3260

McCord JT, Stephens DB, Wilson JL (1991) Validation of flow and transport models for the unsaturated zone toward validating state-dependent macroscopic anisotropy in unsaturated media: field experiments and modeling considerations. J Contam Hydrol 7:145–175

Moore JN, Luoma SN (1990) Hazardous wastes from large-scale metal extraction. A case study. Environ Sci Technol 24:1278–1285

Morel-Seytoux HJ (ed) (1989) Unsaturated flow in hydrologic modeling: theory and practice. Springer, Amsterdam

National Solar Radiation Database (NSRDB) (2016) https://nsrdb.nrel.gov/current-version. Accessed 13 Apr 2016

Navarro MC, Pérez-Sirvent C, Martínez-Sánchez MJ, Vidal J, Tovar PJ, Bech J (2008) Abandoned mine sites as a source of contamination by heavy metals: a case study in a semi-arid zone. J Geochem Explor 96:183–193

Penman HL (1948) Natural evaporation from open water, bare soil and grass. P R Soc Lond A 193:120–145

Radcliffe DE, Šimůnek J (2010) Soil physics with HYDRUS: modeling and applications. CRC Press, Boca Raton

Rassam D, Šimůnek J, van Genuchten MT (2003) Modelling variably saturated flow with HYDRUS-2D. ND Consult, Brisbane

Reynolds WD, Elrick DE (1990) Ponded infiltration from a single ring: I. Analysis of steady flow. Soil Sci Soc Am J 54:1233

Richards LA (1931) Capillary conduction of liquids through porous mediums. J Appl Phys 1:318–333

Salomons W (1995) Environmental impact of metals derived from mining activities: processes, predictions, prevention. J Geochem Explor 52(1–2):5–23

Scanlon BR, Christman M, Reedy RC, Porro I, Šimůnek J, Flerchinger GH (2002) Intercode comparisons for simulating water balance of surficial sediments in semiarid regions. Water Resour Res 38:1323

Scanlon BR, Reedy RC, Keese KE, Dwyer SF (2005) Evaluation of evapotranspirative covers for waste containment in arid and semi-arid regions in the southwestern USA. Vadose Zone J 4:55–71

Schaap MG (2003) Rosetta Lite, v. 1.1. US Salinity Laboratory. Agric Res Serv USDA Riverside Calif

Schaap MG, van Genuchten MT (2006) A modified Mualem–van Genuchten formulation for improved description of the hydraulic conductivity near saturation. Vadose Zone J 5:27–34

Schroeder PR, Dozier TS, Zappi PA, McEnroe BM, Sjostrom JW, Peyton RL (1994) The hydrologic evaluation of landfill performance (HELP) model: engineering documentation for version 3. U.S. Environmental Protection Agency Office of Research and Development, Washington, DC

Shah N, Nachabe M, Ross M (2007) Extinction depth and evapotranspiration from ground water under selected land covers. Groundwater 45:329–338

Šimůnek J, Miroslav Š (2009) Notes on spatial and temporal discretization (when working with HYDRUS). https://www.pc-progress.com/Documents/Notes_on_Spatial_and_Temporal_Discretization.pdf. Acessed 1 June 2016

Šimůnek J, Van Genuchten MT, Šejna M (2012) The HYDRUS Software Package for Simulating the Two-and Three-dimensional Movement of Water, Heat, and Multiple Solutes in Variably-saturated Media; Technical Manual, version 2.0, 230

Šimůnek J, Šejna M, Saito H, Sakai M, van Genuchten MT (2013) The Hydrus-1D software package for simulating the movement of water, heat, and multiple solutes in variably saturated media, version 4.17: HYDRUS Software Series 3. Dept of Environmental Sciences, Univ of California, Riverside

Sisson JB (1987) Drainage from layered field soils: fixed gradient models. Water Resour Res 23:2071–2075

Szymkiewicz A (2013) Modelling water flow in unsaturated porous media: accounting for nonlinear permeability and material heterogeneity. Springer, Berlin, Heidelberg

van Genuchten MT (1980) A closed-form equation for predicting the hydraulic conductivity of unsaturated soils. Soil Sci Soc Am J 44:892–898

Vogel T, van Genuchten MT, Cislerova M (2000) Effect of the shape of the soil hydraulic functions near saturation on variably-saturated flow predictions. Adv Water Resour 24:133–144

Western Regional Climate Center (2016) Pioche, Nevada—climate summary. http://www.wrcc.dri.edu/cgi-bin/cliMAIN.pl?nvpioc. Accessed 17 Jan 2016

White I, Sully MJ (1987) Macroscopic and microscopic capillary length and time scales from field infiltration. Water Resour Res 23:1514–1522

Younger PL, Banwart SA, Hedin RS (2002) Mine water. Springer Netherlands, Dordrecht